

# Soft Gluons and Jets at the LHC

*F. Hautmann*

Theoretical Physics, University of Oxford, Oxford OX1 3NP  
Physics and Astronomy, University of Sussex, Brighton BN1 9QH

We address aspects of jet physics at the Large Hadron Collider focusing on features of recent jet measurements which challenge the theory. We discuss examples illustrating the role of QCD parton showers, nonperturbative corrections, soft multi-gluon emission.

Based on talks given at the conferences *Physics at the LHC 2011* (Perugia, June 2011), *QCD at Cosmic Energies - V* (Paris, June 2012), *ISMD 2012* (Kielce, September 2012)

## 1 Introduction

The first three years of running of the LHC have probed jet physics in new ways, investigating previously unexplored kinematic regions. While next-to-leading-order (NLO) QCD calculations, supplemented with nonperturbative corrections and parton showers, are able to describe well inclusive jet spectra over a wide range of transverse momenta extending from 20 GeV to 2 TeV, several features of LHC jet data challenge the theory. This applies in particular to the behavior of cross sections with increasing rapidity; to correlations of multiple jets in rapidity, azimuthal angle, transverse energy; to non-inclusive observables probing the structure of high multiplicity final states.

This article focuses on aspects of jet production which, despite the presence of a high transverse momentum scale, are sensitive to soft gluon processes and QCD infrared physics. We start with inclusive cross sections in Sec. 2 and discuss the role of parton showering and nonperturbative effects in the context of matched NLO-shower event generators. In Sec. 3 we consider forward jets, and examples of multi-jet correlations. Sec. 4 examines  $b$ -flavor jets. Sec. 5 takes a further look at jet correlations from the viewpoint of multiple parton interactions, emphasizing the role of energy flow variables. Sec. 6 addresses motivation and prospects for extending jet measurements to lower transverse momenta than is presently done.

## 2 Inclusive jet production

Measurements of inclusive jet production are carried out at the LHC [1, 2] over a kinematic range in transverse momentum and rapidity much larger than in any previous collider experiment [3]. Baseline comparisons with Standard Model theoretical predictions rely either on

next-to-leading-order (NLO) QCD calculations, supplemented with nonperturbative (NP) corrections [1, 2] estimated from Monte Carlo event generators, or on NLO-matched parton shower event generators [4, 5]. The upper panels in Fig. 1 [1] report the first kind of comparison, showing that the NLO calculation agrees with data at central rapidities, while increasing deviations are seen with increasing rapidity at large transverse momentum  $p_T$  [1]. The question arises of whether such behavior is associated with higher-order perturbative contributions or with nonperturbative components of the cross section.

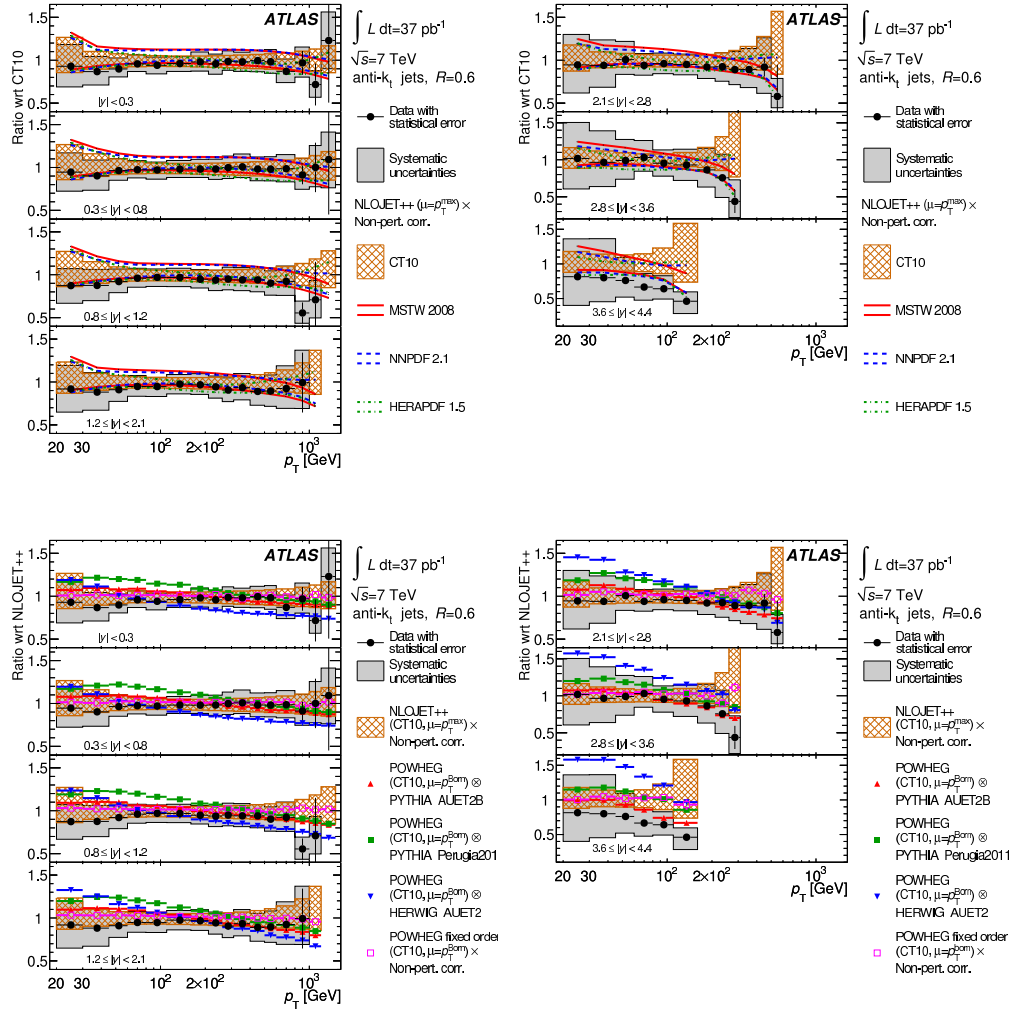


Figure 1: *Inclusive jet spectra* [1] compared with (top) *NLO+NP results* and (bottom) *NLO-matched shower results*.

The lower panels in Fig. 1 [1] show the second kind of comparison based on POWHEG calculations [6], in which NLO matrix elements are matched with parton showers [7, 8]. This improves the description of data, indicating that higher-order radiative contributions taken

into account via parton showers are numerically important. At the same time, the results show large differences between POWHEG calculations interfaced with different shower generators, HERWIG [7] and PYTHIA [8], in the forward rapidity region. This region is sensitive to the details of parton showering corrections.

These observations make it apparent that QCD contributions beyond NLO are essential for the understanding of LHC jet data. In the following subsection we discuss showering and nonperturbative effects.

## 2.1 Nonperturbative and showering corrections

Using leading-order Monte Carlo (LO-MC) generators [7, 8], the nonperturbative correction factors are schematically obtained in [1, 2] as

$$K_0^{NP} = N_{LO-MC}^{(ps+mpi+had)} / N_{LO-MC}^{(ps)} \quad , \quad (1)$$

where  $(ps + mpi + had)$  and  $(ps)$  mean respectively a simulation including parton showers, multiparton interactions and hadronization, and a simulation including only parton showers in addition to the LO hard process.

While this is a natural way to estimate NP corrections from LO+PS event generators, it is noted in [9] that when these corrections are combined with NLO parton-level results a potential inconsistency arises because the radiative correction from the first gluon emission is treated at different levels of accuracy in the two parts of the calculation. To avoid this, Ref. [9] proposes a method which uses NLO Monte Carlo (NLO-MC) generators to determine the correction. In this case one can consistently assign correction factors to be applied to NLO calculations. This method allows one to study separately correction factors to the fixed-order calculation due to parton showering effects. To do this, Ref. [9] introduces the correction factors  $K^{NP}$  and  $K^{PS}$  as

$$K^{NP} = N_{NLO-MC}^{(ps+mpi+had)} / N_{NLO-MC}^{(ps)} \quad , \quad (2)$$

$$K^{PS} = N_{NLO-MC}^{(ps)} / N_{NLO-MC}^{(0)} \quad , \quad (3)$$

where the denominator in Eq. (3) is defined by switching off all components beyond NLO in the Monte Carlo simulation.

The factor  $K^{NP}$  in Eq. (2) differs from  $K_0^{NP}$  because of the different definition of the hard process. In particular the multi-parton interaction  $p_T$  cut-off scale is different in the LO and NLO cases. Numerical results are shown in Fig. 2. The factor  $K^{PS}$  in Eq. (3), on the other hand, is new. It singles out contributions due to parton showering and has not been considered before. Unlike the NP correction, it gives finite effects also at large  $p_T$ . The results in Fig. 3 show in particular that this correction is not merely a rescaling but is  $y$  and  $p_T$  dependent, especially when rapidity is non-central.

The result in Fig. 3 comes from initial-state and final-state showers. These are interleaved so that the combined effect is nontrivial and cannot be obtained by simply adding the two [9]. In general the effect from parton shower is largest at large  $|y|$ , where the initial-state parton shower is mainly contributing at low  $p_T$ , while the final-state parton shower is contributing significantly over the whole  $p_T$  range. It is observed in [9] that the main initial-state showering effect comes from kinematical shifts in longitudinal momentum distributions [10], due to combining collinearity approximations with the Monte Carlo implementation of energy-momentum conservation constraints. The effect of the kinematic shifts is illustrated in Fig. 4 [9], showing

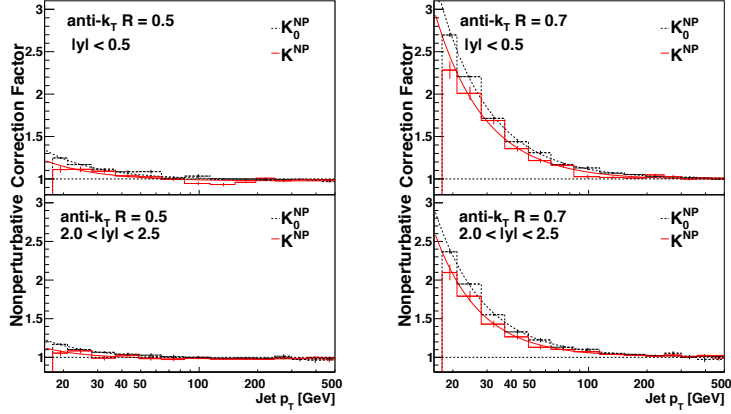


Figure 2: The NP correction factors to jet transverse momentum distributions obtained from Eq. (1) and Eq. (2), using PYTHIA and POWHEG respectively, for  $|y| < 0.5$  and  $2 < |y| < 2.5$ . Left:  $R = 0.5$ ; Right:  $R = 0.7$ . [9]

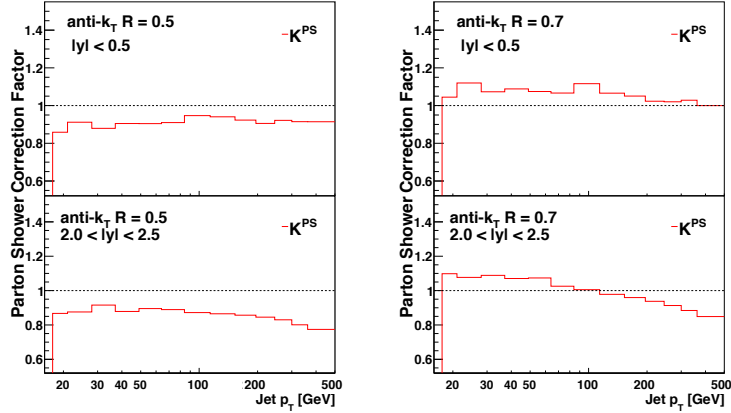


Figure 3: The parton shower correction factor to jet transverse momentum distributions, obtained from Eq. (3) using POWHEG for  $|y| < 0.5$  and  $2 < |y| < 2.5$ . Left:  $R = 0.5$ ; Right:  $R = 0.7$ . [9]

the distribution in the parton longitudinal momentum fraction  $x$  before parton showering and after parton showering. We see that the longitudinal shift is negligible for central rapidities but becomes significant for  $y > 1.5$ .

In summary, the nonperturbative correction factor  $K^{NP}$  introduced from NLO-MC in Eq. (2) gives non-negligible differences compared to the LO-MC contribution [1, 2] at low to intermediate jet  $p_T$ , while the showering correction factor  $K^{PS}$  of Eq. (3) gives significant effects over the whole  $p_T$  range and is largest at large jet rapidities  $y$ . Because of this  $y$  and  $p_T$  dependence, taking properly into account NP and showering correction factors changes the shape of jet distributions, and may thus influence the comparison of theory predictions with experimental data. We anticipate in particular that taking account of the showering correction factor will be relevant in fits for parton distribution functions using inclusive jet data.

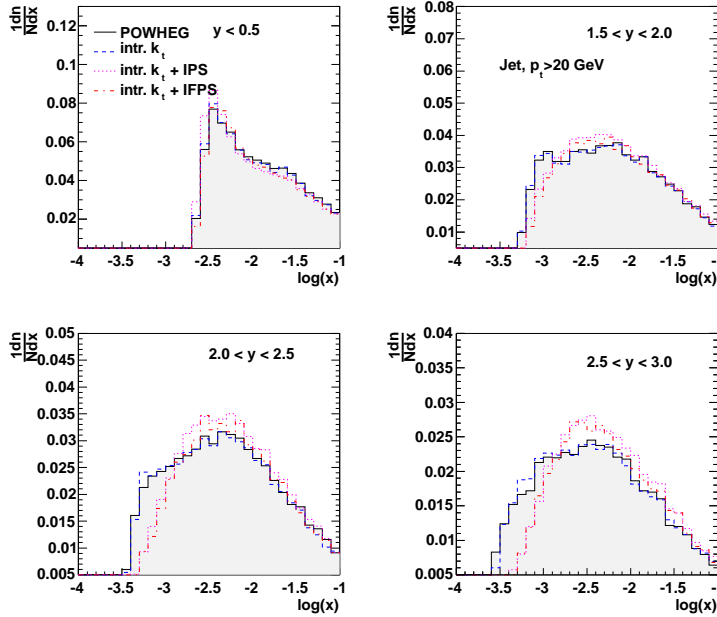


Figure 4: *Distributions in the parton longitudinal momentum fraction  $x$  before (POWHEG) and after parton showering (POWHEG+PS), for inclusive jet production at different rapidities for jets with  $p_T > 18$  GeV obtained by the anti- $k_t$  jet algorithm [11] with  $R = 0.5$ . Shown is the effect of intrinsic  $k_t$ , initial (IPS) and initial+final state (IFPS) parton shower. [9]*

### 3 Forward jets

A program of jet physics in the forward region can be carried out for the first time at the LHC [12], by exploiting the large phase space opening up at high center-of-mass energies, and the unprecedented reach in rapidity of the experimental instrumentation [13]. First forward jet measurements have been performed by LHC experiments [14, 15, 16].

The evaluation of QCD theoretical predictions for forward jets is made complex by high- $p_T$  production occurring in a region characterized by multiple hard scales, possibly widely disparate from each other [12]. In addition to the parton-shower kinematic effects discussed in Sec. 2, when jets are measured at large separations in rapidity dynamical contributions from soft multi-gluon radiation [17, 18, 19] set in, calling for perturbative resummations of large-rapidity logarithms to all orders in  $\alpha_s$ . This motivates current studies based on the BFKL equation [20, 21, 22, 23]. Furthermore, with increasing rapidities the nonperturbative parton distributions are probed in highly asymmetric kinematic regions near the boundaries  $x \rightarrow 0$  and  $x \rightarrow 1$  of partonic phase space [12, 19]. This in turn implies that contributions from multiple parton collisions [24, 25] are potentially enhanced [26, 27, 28]. Effects of multiple scatterings may be studied in di-jet as well as di-hadron spectra [29], in pp collisions and in collisions of light [30] and heavy [31, 32, 33] nuclei.

Forward jets enter the LHC physics program in an essential way both for new particle discovery processes (e.g., Higgs searches [34] in vector boson fusion channels, jet studies in decays of highly boosted heavy states [35]) and for new aspects of standard model physics (e.g., small- $x$  QCD and its interplay with cosmic ray physics [36, 37], studies of high-density parton matter [38, 39]). The first forward jet measurements [14, 15, 16] show that, while inclusive forward jet spectra are roughly in agreement with predictions from different Monte Carlo simulations, detailed aspects of production rates and correlations are not well understood yet. Recent phenomenological analyses are carried out in [40, 41].

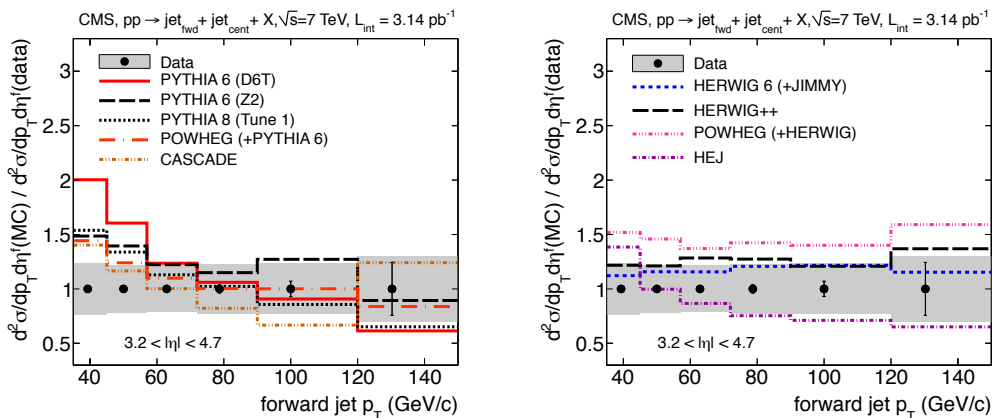


Figure 5: Ratio theory/data [14] for dijet events with a central and a forward jet as a function of the forward jet transverse momentum.

An example is given by the di-jet observables [42] associated with events containing a forward and a central jet. Experimental measurements and Monte Carlo comparisons are shown in Fig. 5 [14]. The results indicate that none of the Monte Carlo generators describes the data well in all regions; in particular NLO-matched calculations from POWHEG give large differences in the forward jet  $p_T$  distribution when combined with different parton showers, see POWHEG+HERWIG vs. POWHEG+PYTHIA.

In [42, 43] this behavior is investigated by studying  $\Delta R$  jet distributions designed to provide

a measure, in azimuth and rapidity space, of the extent to which jets are dominated by hard partons in the matrix element or originate from showering. Large contribution to jets from showering are found [42] in the case of asymmetric parton kinematics, i.e, when one of the initial-state showers goes down to small  $x$ . Ref. [43] furthers this study by considering the central jet transverse energy spectrum, in di-jet events with a central and a forward jet, using the NLO event generator POWHEG matched with parton showers PYTHIA and HERWIG. Fig. 6 [43] shows results for the two cases, normalized to the result obtained by switching off parton showering. The marked differences between the two cases are consistent with the findings in [14], and with the large contribution to jets from showering found in [42]. In particular in the forward-central events considered high-rapidity correlations turn out to affect the behavior of jet distributions in the central region.

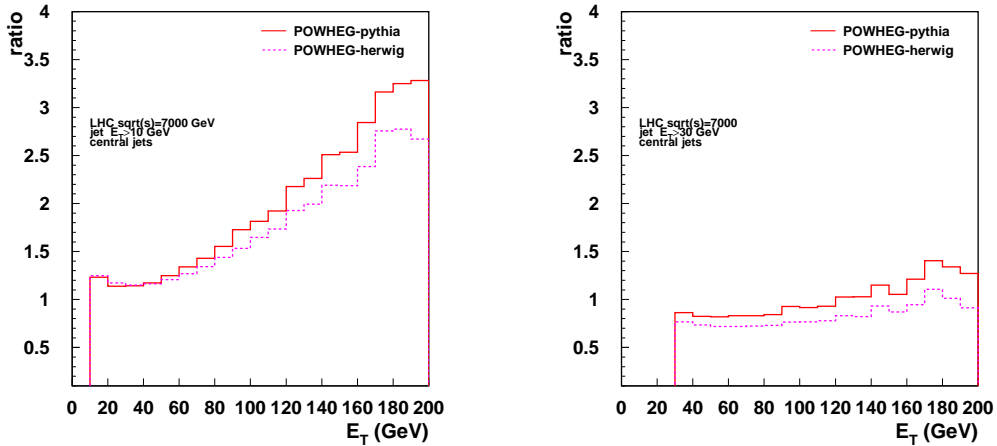


Figure 6: *Ratio of NLO+shower to no-shower results for dijet events with a central and a forward jet as a function of the central jet transverse momentum [43]. (left)  $E_T > 10$  GeV; (right)  $E_T > 30$  GeV.*

A classic test of QCD high-energy resummation for jets at large rapidity separations [17] is given by the azimuthal decorrelation between jets. Fig. 7 [42] shows the cross section as a function of the azimuthal distance  $\Delta\phi$  between central and forward jets reconstructed with the Siscone algorithm [44] ( $R = 0.4$ ), for different rapidity separations. It shows results computed by PYTHIA Monte Carlo [45], with and without multiparton interactions, and by CASCADE Monte Carlo [46], which includes small- $x$  gluon coherence effects [47] in the initial-state shower. The main point is that the decorrelation as a function of  $\Delta\eta$  increases in CASCADE as well as in PYTHIA, respectively as a result of finite-angle gluon radiation in single-chain parton shower or as a result of multiple-chain collinear showers; but while in the low  $E_T$  region (Fig. 7 (left)) this is similar between CASCADE and PYTHIA with multiparton interactions for  $\Delta\eta < 4$ , in the higher  $E_T$  region (Fig. 7 (right)) the influence of multiparton interactions in PYTHIA is small and CASCADE predicts everywhere a larger decorrelation. We will come back to this and discuss correlations further in Sec. 5 from the point of view of energy flow observables.

While the specific results shown in this section refer to forward-central jet correlations, it is interesting to consider extensions to the forward-backward kinematics. This will allow one to address the large- $\Delta y$  di-jet data sets [15, 16], currently rather poorly understood; to search

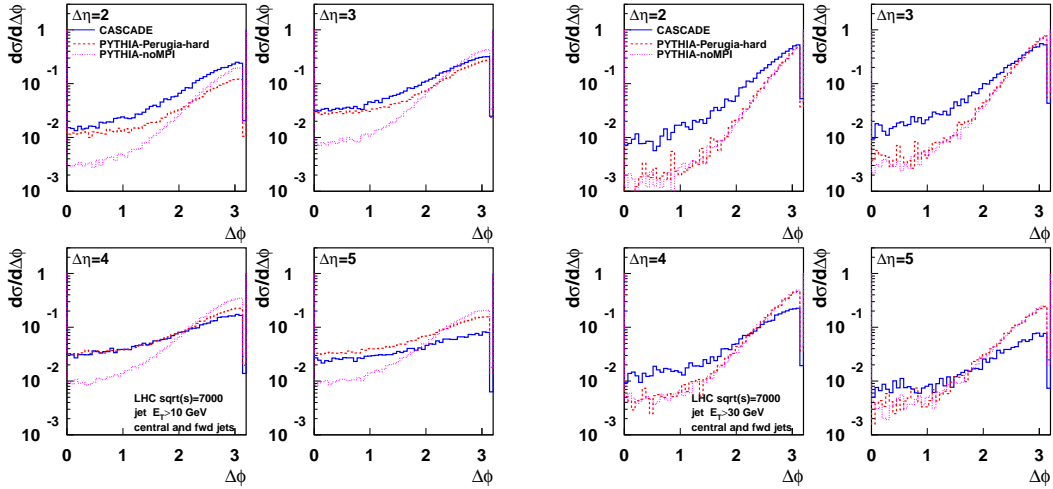


Figure 7: Cross section versus azimuthal distance  $\Delta\phi$  between central and forward jet, at different rapidity separations  $\Delta\eta$ , for jets with transverse energy  $E_T > 10$  GeV (left) and  $E_T > 30$  GeV (right) [42].

for Mueller-Navelet effects [17]; to analyze backgrounds in Higgs boson studies [34] from vector boson fusion channels. In particular, one may be able to extract information on Higgs properties and couplings from jet kinematics [48]. In this case too finite-angle radiative contributions to single-chain showers, extending across the whole rapidity range, affect the underlying jet activity accompanying the Higgs [49] and may give competing effects to multiple-parton interactions.

## 4 $B$ -jets

Some of the features observed for inclusive jets in Sec. 2 are also present in  $b$ -flavor jets [50, 51]. Fig. 8 [50] shows a comparison of the measured  $B$ -jet transverse momentum spectra with matched NLO-shower calculations using MC@NLO [52]. The description of the data is generally good at central rapidities, while at large  $y$  and large  $p_T$  the Monte Carlo is above the data. Similar behavior is shown by comparisons with POWHEG [53] in [51].

Fig. 9 [9] studies kinematic corrections to  $B$ -jet production due to longitudinal momentum shifts in the initial-state parton shower, similar to those discussed for inclusive jets in Fig. 4. For  $B$ -jets in different rapidity regions [50], the gluon  $x$  distribution is plotted from POWHEG before parton showering and after including various components of the parton shower generator, using the PYTHIA parton shower Z2 [54] (including hadronization components to identify  $B$ -jets). Fig. 9 shows similar shifts in longitudinal momentum with increasing rapidity as in the inclusive jet case. A better understanding of  $B$  production in this region will affect studies of the Higgs to  $b\bar{b}$  decay channel, e.g. in the associated production with vector bosons.

Although the explicit calculations in Fig. 9 are performed using a particular NLO-shower matching scheme (POWHEG), the effect is common to any calculation matching NLO with collinear showers. As discussed in [9, 10], the kinematic shifts due to the momentum reshuffling can affect predictions of matched NLO-shower calculations both through the perturbative

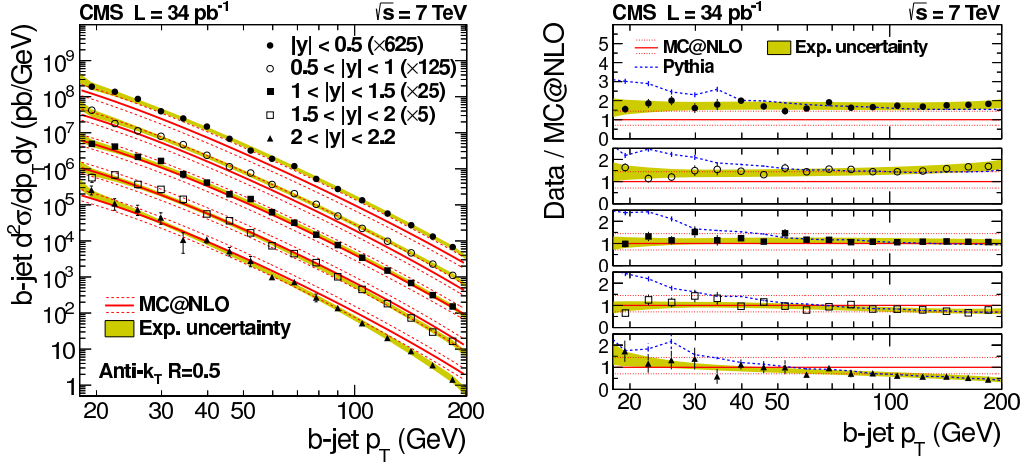


Figure 8: Inclusive  $B$ -jet spectra [50].

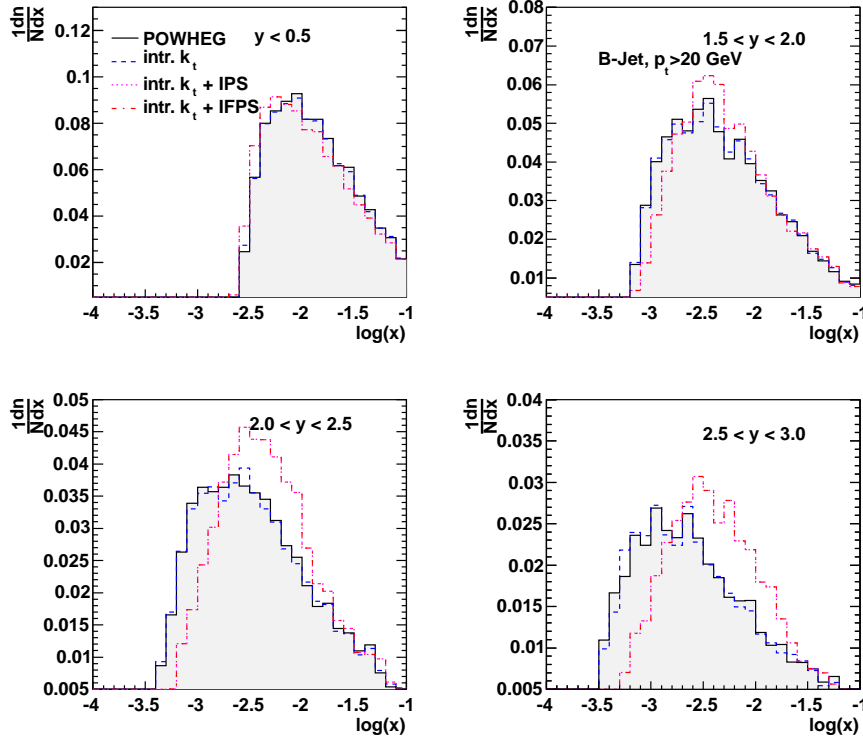


Figure 9: Production of  $B$ -jets: distribution in the parton longitudinal momentum fraction  $x$ , before and after parton showering, for different rapidity regions. Shown is the effect of intrinsic  $k_t$ , initial (IPS) and initial+final state (IFPS) parton shower. [9]

weight for each event and through the evaluation of the parton distribution functions. In calculations using integrated parton density functions this implies that correction factors as discussed in Sec. 2 have to be applied after the evaluation of the cross section. On the other hand, we note that this is avoided in approaches using transverse momentum dependent pdfs [55, 56, 57, 58] from the beginning (TMDs or uPDFs). It will thus be of interest to study it quantitatively in Monte Carlo generators which implement these pdfs [46, 59, 60].

We note further that helicity amplitudes techniques are being developed [61] for multi-leg processes with up to two off-shell gluons in the high-energy limit [18], and applied to complex final states containing heavy quarks [62], including  $b\bar{b}$  + jets and  $b\bar{b}$  + vector bosons. Once combined with TMD pdfs and parton showers, these multi-parton amplitudes can provide a computational tool to overcome the limitations of collinear approximations, and take into account both kinematical and dynamical effects associated with multiple-scale processes.

## 5 Multi-parton interactions and energy flow variables

Besides jet cross sections, event shape variables are studied at the LHC [63, 64] and used to characterize the events' energy flow and the structure of multi-jet final states. Baseline descriptions of multi-jet events are obtained by methods merging parton showers and multi-leg hard matrix elements [5]. First measurements of LHC hadronic event shapes [63] point to parton showering effects dominating over contributions from hard matrix elements evaluated at high multiplicity. Jet shape variables describing the jet's internal structure and the energy flow within a jet are also studied [65]. These observables are used in searches for potential new physics signals from decays of massive states in the boosted regime [35], or away from it [66]. Besides jet substructure, such observables are sensitive to soft physics effects, including underlying events, pile-up, multiple parton interactions [26].

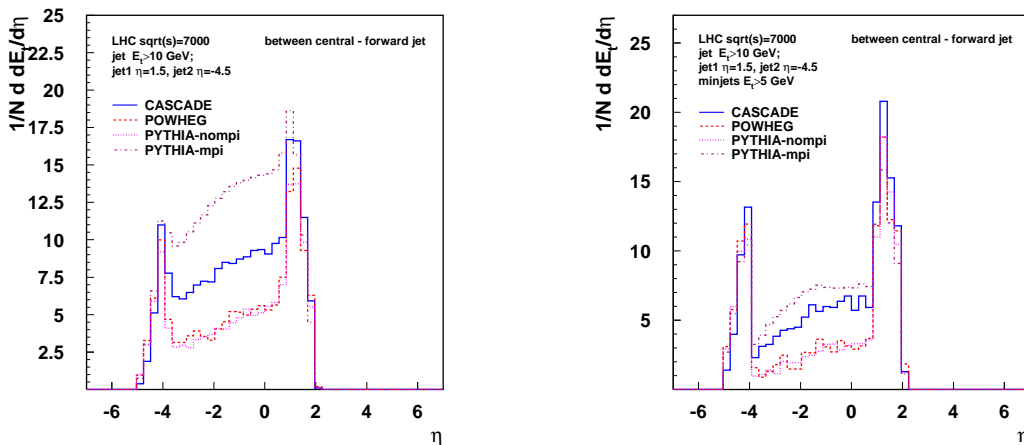


Figure 10: *Transverse energy flow [70] in the inter-jet region: (left) particle flow; (right) mini-jet flow.*

Energy flow measurements [67] in minimum bias and dijet events, designed to investigate properties of the soft underlying event, emphasize the difficulty [68] in achieving a unified

underlying event description from central to forward rapidities, based on PYTHIA [45] Monte Carlo tuning. Forward-backward correlations [69] in minimum bias may help analyze the event structure. Complementary to the above measurements are transverse energy flow observables associated with the production of jets widely separated in rapidity [70], sensitive to harder color radiation, and useful for studies of showering and of multi-parton interactions [71]. The transverse energy flow may be defined by summing the energies over all particles in the final states above a minimum  $E_T$ , or alternatively [70] by first clustering particles into jets by means of a jet algorithm, and then constructing the associated energy flow from jets with transverse energy above a given lower bound  $q_0$ . In the latter case one measures a (mini)jet energy flow, and infrared safety is ensured by the use of the clustering algorithm.

Figs. 10 and 11 report results for the particle and minijet energy flow associated with production of central and forward jets [70] from three Monte Carlo event generators: the  $k_{\perp}$ -shower CASCADE generator [46], to evaluate contributions of high-energy logarithmic corrections; the NLO matched POWHEG generator [6], to evaluate the effects of NLO corrections to matrix elements; PYTHIA Monte Carlo [45], used in two different modes: with the LHC tune Z1 [54] (PYTHIA-mpi) to evaluate contributions of multi-parton interactions, and without any multi-parton interactions (PYTHIA-nompi).

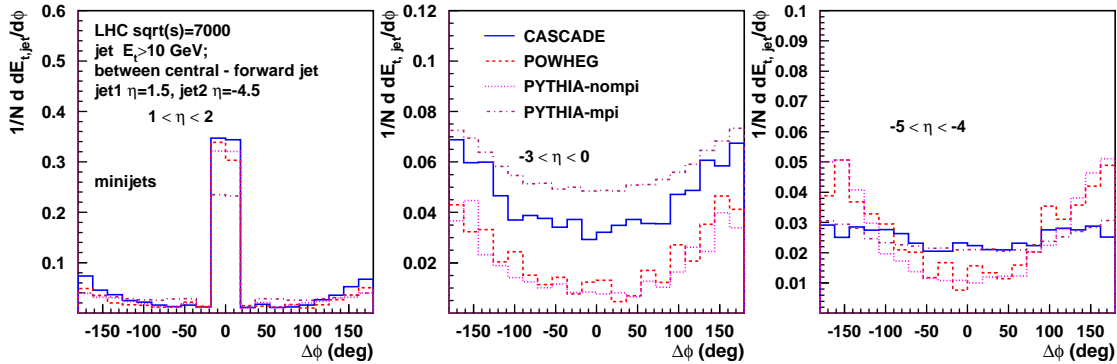


Figure 11: Azimuthal dependence of the mini-jet energy flow [70] for different rapidity ranges: (left) central-jet; (middle) intermediate; (right) forward-jet.

Fig. 10 shows the pseudorapidity dependence of the transverse energy flow in the region between the central and forward jets. The particle energy flow plot on the left in Fig. 10 shows the jet profile picture, and indicates enhancements of the energy flow in the inter-jet region with respect to the PYTHIA-nompi result from higher order emissions in CASCADE and from multiple parton collisions in PYTHIA-mpi. On the other hand, there is little effect from the next-to-leading hard correction in POWHEG with respect to PYTHIA-nompi. The energy flow is dominated by multiple-radiation, parton-shower effects. The mini-jet energy flow plot on the right in Fig. 10 indicates similar effects, with reduced sensitivity to infrared radiation. As the mini-jet flow definition suppresses the contribution of soft radiation, the CASCADE and PYTHIA-mpi results become more similar in the inter-jet region. Distinctive effects are also found in [70] by computations in the region away from the jets.

Fig. 11 illustrates the azimuthal dependence of the mini-jet transverse energy flow. Here  $\Delta\phi$  is measured with respect to the central jet. The  $\Delta\phi$  distribution is shown for three different

rapidity ranges, corresponding to the central-jet, forward-jet, and intermediate rapidities. As we go toward forward rapidity, the CASCADE and PYTHIA-mpi calculations give a more pronounced flattening of the  $\Delta\phi$  distribution compared to POWHEG and PYTHIA-nompi, corresponding to increased decorrelation between the jets.

The above numerical results indicate that soft, finite-angle multi-gluon emission over large rapidity intervals gives sizeable contribution to the inter-jet energy flow. Non-collinear corrections to single-chain showering may in particular influence the rates for multi-parton interactions [26]. This also underlines the relevance of approaches which aim at a more complete description of initial state dynamics by generalizing the notion of parton distributions [56, 57], both for quark-dominated [72] and gluon-dominated [73] processes. It will be of interest to extend energy flow studies using different triggers, e.g. vector boson + jet [74] at large rapidity, which may help constrain multiple interaction rates [45, 54, 75].

## 6 Towards low $p_T$

Hadron jets are measured at the LHC over a wide range in transverse momenta from 20 GeV to a few TeV. It is of interest to explore to what extent the picture of jets provided by the algorithms used for jet reconstruction (and corresponding shower Monte Carlo event simulations) can be pushed towards the semi-soft region of lower transverse momenta. As discussed earlier, low- $p_T$  jets may be used to investigate QCD physics at small  $x$ . A jet-like description of low- $p_T$  hadronic final states may provide insight into the region where the LHC has produced striking evidence [76] of long-range di-hadron correlations in high multiplicity events.

It has been observed in [77] that if jet measurements at the LHC are extended down to transverse momenta of the order of a few GeV one can define a visible leading jet cross section sensitive to the unitarity bound set by the inelastic proton-proton rate which has recently been measured [78, 79, 80]. This can be done within the range of acceptance of the measurement without using any extrapolation [77]. Because of the low transverse momenta, this will rely primarily on jets constructed from charged tracks. Given the decay in particle tracking capabilities with increasing rapidity, one may focus on the central pseudorapidity range.

The main interest of these measurements is the possibility to investigate the leading jet cross section near the  $p_T$  region,  $p_T = \mathcal{O}$  (a few GeV), where the inelastic pp production rate is saturated [77]. At the LHC, for the first time in collider experiments, this occurs in the weakly coupled region. Even though at weak coupling, dynamical effects slowing down the rise of the cross section in this region involve strong fields and non-perturbative physics. In order to analyze the saturation region, Ref. [77] introduces an event cross section, defined as an integral over the differential leading jet cross section, which does not depend on the jet multiplicity. Fig. 12 shows the visible jet cross section using PYTHIA [8] with jets reconstructed by the anti- $k_T$  algorithm [11] for  $R = 0.5$  down to low transverse momenta.

In Fig. 12 (left) the perturbative result reaches the inelastic bound [78] for minimum  $p_T \simeq 4$  GeV. In the region just above this value,  $p_T = \mathcal{O}(10)$  GeV, effects responsible for the taming of the cross section set in. Fig. 12 (right) shows the cross section based on the model [25, 81], in which the rise of the cross section is tamed at small values of  $p_T$  by introducing a  $p_{T0}$  cut-off parameter obtained from fits to describe measurements of the underlying event.

Fig. 13 [77] shows a comparison of the jet cross section for  $p_{T0} = 0$ , including parton shower and hadronization, with the cross section obtained from PYTHIA including the  $p_{T0}$  model. In Fig. 13 (right) we show the effect of multi-parton interactions. Especially in the region of

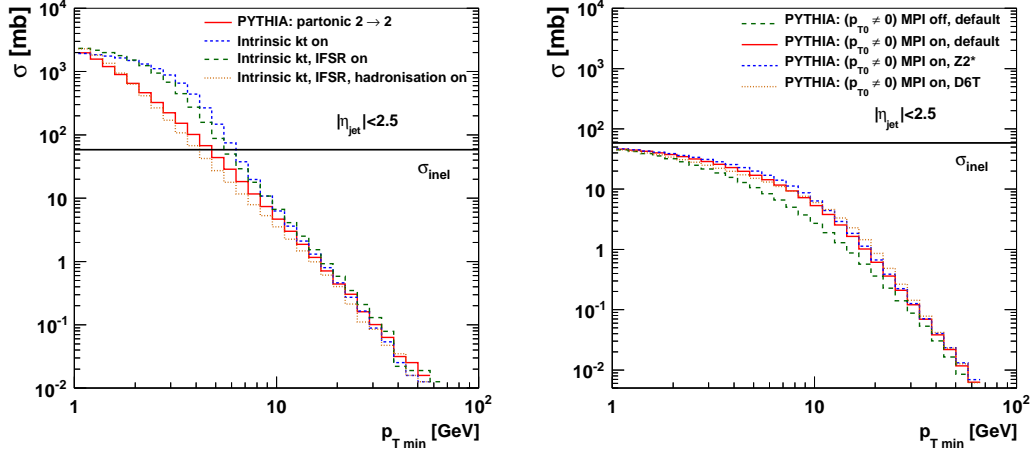


Figure 12: (Left) Cross section from purely partonic  $2 \rightarrow 2$  process, including intrinsic  $k_t$ -effects, including initial and final state parton showers (IFSR) and finally hadronisation. (Right) predicted cross section applying  $p_{T0} \neq 0$  and MPI with different underlying event tunes of PYTHIA. [77]

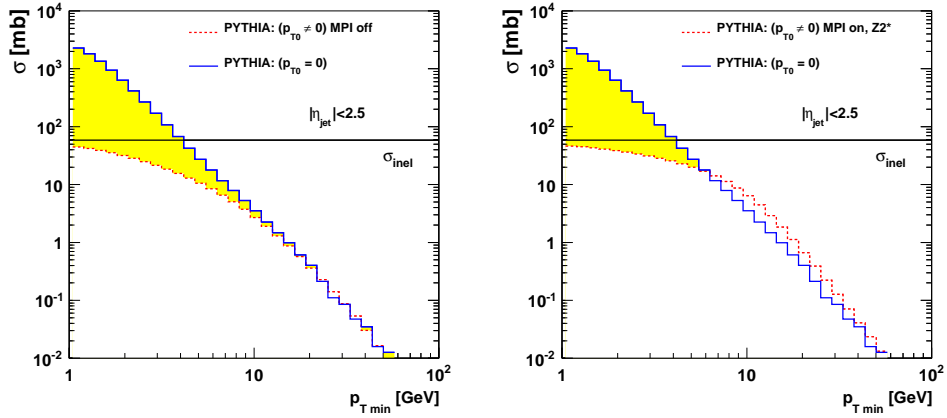


Figure 13: The cross section [77] as a function of  $p_{Tmin}$  as predicted by PYTHIA in the range  $|\eta| < 2.5$ . The solid (blue) line shows the prediction applying  $p_{T0} = 0$  including parton shower and hadronisation, while the dashed (red) line shows the prediction with  $p_{T0} \neq 0$ ; (left) is without multi-parton interactions, (right) including multi-parton interactions with tune  $Z2^*$  [54].

$p_T < 10$  GeV a clear deviation from the  $p_{T0} = 0$  prediction is visible. Measuring the jet cross section in this range would probe the transition from the large- $p_T$  perturbative behavior to the medium to low  $p_T$  region where (weak-coupling) unitarity corrections set in. We note that the analysis [82] already illustrates the feasibility of measuring jets at low  $p_T$ . However, event cross sections such as that described above to study unitarity have not yet been examined. Results from different Monte Carlo models in [82] are effectively normalized to the lowest  $p_T$  bin.

Besides  $pp$  collisions, low  $p_T$  jet measurements are relevant in pA and AA nuclear collisions. If the inelastic cross section is measured in AA and pA, they may be useful to characterize properties of final states in terms of jets or flows [83], and investigate transverse momentum dependent dynamics and multi-parton interactions [84, 85].

Compared to the collinearly-factorized cut-off model [25, 81], a physically different picture of the turn-over region is provided by approaches based on TMD initial-state distributions [56, 58, 86] incorporating small- $x$  gluon coherence [47]. In this case the rise of the cross section is slowed down by finite transverse momenta in the initial state. The effect of combining this with nonlinear terms in the evolution of parton cascades [87] and the dependence of the turn-over region on the infrared behavior of the strong coupling [88] warrant investigations. Extending jet definition and measurements to the region of low transverse momenta may give us radically new information on the underlying physical picture of high-energy multi-particle production.

## 7 Conclusion

Jets enter in essentially all areas of the LHC physics program, from new particle discovery processes to precision studies of the Standard Model to searches for physics beyond the Standard Model. Experimental results in the first three years of running of the LHC have provided us not only with solid confirmation of our understanding of jet physics from QCD but also with challenges and surprises. These involve both the high- $p_T$  region, featuring several new effects of QCD parton showers, and the low- $p_T$  region, probing nonperturbative components of jet cross sections. Much is to be learnt about the theory of hadronic jets and its applications to precision phenomenology as forthcoming LHC data analyses and measurements keep exploring jets in new regions of phase space and probing different sectors of QCD.

**Acknowledgements.** The material presented in this article originated from discussion and collaboration with many people, in particular S. Dooling, D. d’Enterría, A. Grebenyuk, P. Gunnellini, M. Deak, H. Jung, M. Hentschinski, N. McCubbin, Z. Nagy, P. Katsas, A. Knutsson, K. Kutak, K. Rabbertz, C. Roda.

## References

- [1] ATLAS Coll. (G. Aad et al.), Phys. Rev. D **86** (2012) 014022.
- [2] CMS Coll. (S. Chatrchyan et al.), Phys. Rev. Lett. **107** (2011) 132001; arXiv:1212.6660 [hep-ex].
- [3] K. Rabbertz, review talk at ISMD 2012, Kielce, September 2012.
- [4] P. Nason and B.R. Webber, Ann. Rev. Nucl. Part. Sci. **62** (2012) 187.
- [5] S. Höche, SLAC preprint SLAC-PUB-14498 (2011); S. Höche and M. Schönherr, Phys. Rev. D **86** (2012) 094042.
- [6] S. Alioli, K. Hamilton, P. Nason, C. Oleari and E. Re, JHEP **1104** (2011) 081.
- [7] G. Corcella *et al.*, JHEP **0101** (2001) 010 [arXiv:hep-ph/0011363]; G. Corcella *et al.*, arXiv:hep-ph/0210213.

- [8] T. Sjöstrand, S. Mrenna and P. Skands, *JHEP* **0605** (2006) 026.
- [9] S. Dooling, P. Gunnellini, F. Hautmann and H. Jung, arXiv:1212.6164 [hep-ph]; arXiv:1304.7180 [hep-ph].
- [10] F. Hautmann and H. Jung, *Eur. Phys. J. C* **72** (2012) 2254; *Nucl. Phys. Proc. Suppl.* **234** (2013) 51.
- [11] M. Cacciari, G. Salam and G. Soyez, *JHEP* **0804** (2008) 063.
- [12] F. Hautmann, *Nuovo Cim.* **C32** N5-6 (2009) 167 [arXiv:0909.1250 [hep-ph]], *Proc. 23rd Rencontres de Physique de la Vallée d'Aoste (La Thuile, March 2009)*.
- [13] Z. Ajaltouni et al., arXiv:0903.3861 [hep-ph].
- [14] CMS Coll. (S. Chatrchyan et al.), *JHEP* **1206** (2012) 036.
- [15] ATLAS Coll. (G. Aad et al.), *JHEP* **1109** (2011) 053.
- [16] CMS Coll. (S. Chatrchyan et al.), *Eur. Phys. J. C* **72** (2012) 2216.
- [17] A.H. Mueller and H. Navelet, *Nucl. Phys.* **B282** (1987) 727; A.H. Mueller, *Nucl. Phys. B Proc. Suppl.* **18C** (1990) 125; S. Catani, M. Ciafaloni and F. Hautmann, *Nucl. Phys. B Proc. Suppl.* **29A** (1992) 182; C. Ewerz, L.H. Orr, W.J. Stirling and B.R. Webber, *J. Phys.* **G26** (2000) 696.
- [18] S. Catani et al., *Phys. Lett.* **B242** (1990) 97; *Nucl. Phys.* **B366** (1991) 135; *Phys. Lett.* **B307** (1993) 147; *Phys. Lett.* **B315** (1993) 157; *Nucl. Phys.* **B427** (1994) 475.
- [19] M. Deak, F. Hautmann, H. Jung and K. Kutak, *JHEP* **0909** (2009) 121; arXiv:0908.1870 [hep-ph].
- [20] D. Colferai, F. Schwennsen, L. Szymanowski and S. Wallon, *JHEP* **1012** (2010) 026; arXiv:1110.1250 [hep-ph]; B. Ducloué, L. Szymanowski and S. Wallon, arXiv:1208.6111 [hep-ph]; arXiv:1302.7012 [hep-ph].
- [21] J.R. Andersen, T. Hapola and J.M. Smillie, *JHEP* **1209** (2012) 047; J.M. Smillie, arXiv:1209.4312 [hep-ph], J.R. Andersen and J.M. Smillie, *JHEP* **1106** (2011) 010, *Phys. Rev.* **D81** (2010) 114021.
- [22] G. Chachamis, M. Hentschinski, J.D. Madrigal Martinez and A. Sabio Vera, arXiv:1212.4992 [hep-ph]; arXiv:1211.2050 [hep-ph]; M. Hentschinski and A. Sabio Vera, *Phys. Rev.* **D85** (2012) 056006.
- [23] F. Caporale, D.Yu. Ivanov, B. Murdaca and A. Papa, arXiv:1211.7225 [hep-ph]; arXiv:1209.6233 [hep-ph]; F. Caporale et al., arXiv:1212.0487 [hep-ph]; *JHEP* **1202** (2012) 101.
- [24] N. Paver and D. Treleani, *Nuovo Cim.* **A70** (1982) 215.
- [25] T. Sjöstrand and M. van Zijl, *Phys. Rev.* **D36** (1987) 2019.
- [26] P. Bartalini and L. Fanò (eds.), *Proc. 1st MPI Workshop (Perugia, 2008)*, arXiv:1003.4220 [hep-ex]; P. Bartalini et al., arXiv:1111.0469 [hep-ph].
- [27] Yu.L. Dokshitzer, arXiv:1203.0716 [hep-ph]; B. Blok, Yu.L. Dokshitzer, L. Frankfurt and M. Strikman, arXiv:1206.5594 [hep-ph]; *Eur. Phys. J. C* **72** (2012) 1963, *Phys. Rev.* **D83** (2011) 071501.
- [28] M. Diehl, arXiv:1111.0272 [hep-ph]; M. Diehl, D. Ostermeier and A. Schäfer, *JHEP* **1203** (2012) 089.
- [29] K. Dusling and R. Venugopalan, arXiv:1302.7018 [hep-ph]; *Phys. Rev.* **D87** (2013) 051502.
- [30] G. Calucci and D. Treleani, *Phys. Rev.* **D86** (2012) 036003; *Phys. Rev.* **D83** (2011) 016012.
- [31] J.L. Albacete, A. Dumitru and C. Marquet, arXiv:1302.6433 [hep-ph].
- [32] K. Kutak and S. Sapeta, *Phys. Rev.* **D86** (2012) 094043.
- [33] F. Dominguez, C. Marquet, B.W. Xiao and F. Yuan, *Phys. Rev.* **D83** (2011) 105005.
- [34] CMS Coll. (S. Chatrchyan et al.), *Phys. Lett.* **B713** (2012) 68; *Phys. Lett.* **B710** (2012) 403; ATLAS Coll. (G. Aad et al.), *Phys. Rev. Lett.* **108** (2012) 111803; *JHEP* **1209** (2012) 070.
- [35] A. Altheimer et al., *J. Phys.* **G39** (2012) 063001.
- [36] D. d'Enterria, R. Engel, T. Pierog, S. Ostapchenko and K. Werner, *Few Body Syst.* **53** (2012) 173; *As-tropart. Phys.* **35** (2011) 98.
- [37] M. Grothe, F. Hautmann and S. Ostapchenko, arXiv:1103.6008 [hep-ph].
- [38] E. Iancu, arXiv:1205.0579 [hep-ph].
- [39] D. d'Enterria, arXiv:0911.1273 [hep-ex].
- [40] S. Alioli, J.R. Andersen, C. Oleari, E. Re and J.M. Smillie, *Phys. Rev.* **D85** (2012) 114034.
- [41] Y. Hatta, C. Marquet, C. Royon, G. Soyez, T. Ueda and D. Werder, arXiv:1301.1910 [hep-ph].

- [42] M. Deak et al., arXiv:1012.6037 [hep-ph]; F. Hautmann, PoS ICHEP2010 (2010) 108; arXiv:1101.2656.
- [43] M. Deak et al., arXiv:1206.7090 [hep-ph].
- [44] G.P. Salam and G. Soyez, JHEP **0705** (2007) 086; M. Cacciari, G.P. Salam and G. Soyez, <http://fastjet.fr>.
- [45] P. Skands, Phys. Rev. D **82** (2010) 074018.
- [46] H. Jung et al., Eur. Phys. J. C **70** (2010) 1237.
- [47] M. Ciafaloni, Nucl. Phys. B **296** (1988) 49, S. Catani, F. Fiorani and G. Marchesini, Nucl. Phys. B **336** (1990) 18, G. Marchesini and B.R. Webber, Nucl. Phys. B **386** (1992) 215; F. Hautmann and H. Jung, JHEP **0810** (2008) 113; arXiv:0808.0873 [hep-ph]; arXiv:0804.1746 [hep-ph].
- [48] A. Djouadi, R.M. Godbole, B. Mellado and K. Mohan, arXiv:1301.4965 [hep-ph].
- [49] M. Deak et al., arXiv:1006.5401 [hep-ph]; F. Hautmann, H. Jung and V. Pandis, arXiv:1011.6157 [hep-ph]; F. Hautmann, arXiv:0909.1240; Phys. Lett. B **535** (2002) 159; R.D. Ball et al., arXiv:1303.3590 [hep-ph].
- [50] CMS Coll. (S. Chatrchyan et al.), JHEP **1204** (2012) 084.
- [51] ATLAS Coll. (G. Aad et al.), Eur. Phys. J. C **71** (2011) 1846.
- [52] S. Frixione, P. Nason and B.R. Webber, JHEP **0308** (2003) 007.
- [53] S. Frixione, P. Nason and G. Ridolfi, JHEP **0709** (2007) 126.
- [54] R.D. Field, arXiv:1010.3558 [hep-ph].
- [55] J.C. Collins, *Foundations of perturbative QCD*, CUP 2011.
- [56] E. Avsar, arXiv:1203.1916 [hep-ph]; arXiv:1108.1181 [hep-ph].
- [57] S. Mert Aybat and T.C. Rogers, Phys. Rev. D **83** (2011) 114042.
- [58] F. Hautmann, Acta Phys. Polon. B **40** (2009) 2139; Phys. Lett. B **655** (2007) 26; F. Hautmann and H. Jung, arXiv:0712.0568 [hep-ph]; in J. Bartels et al., arXiv:0902.0377 [hep-ph], Proc. ISMD2008; F. Hautmann, M. Hentschinski and H. Jung, Nucl. Phys. B **865** (2012) 54; arXiv:1205.6358; arXiv:1209.6305.
- [59] H. Jung et al., arXiv:1206.1796 [hep-ph].
- [60] S. Jadach, M. Jezabek, A. Kusina, W. Placzek and M. Skrzypek, Acta Phys. Polon. B **43** (2012) 2067; S. Jadach and M. Skrzypek, Acta Phys. Polon. B **40** (2009) 2071.
- [61] A. van Hameren, P. Kotko and K. Kutak, JHEP **1212** (2012) 029.
- [62] A. van Hameren, P. Kotko and K. Kutak, JHEP **1301** (2013) 078.
- [63] CMS Coll. (V. Khachatryan et al.), Phys. Lett. B **699** (2011) 48.
- [64] ATLAS Coll. (G. Aad et al.), Eur. Phys. J. C **72** (2012) 2211.
- [65] ATLAS Coll. (G. Aad et al.), JHEP **1205** (2012) 128; Phys. Rev. D **83** (2011) 052003; CMS Coll. (S. Chatrchyan et al.), JHEP **1206** (2012) 160.
- [66] M. Gouzevitch, A. Oliveira, J. Rojo, R. Rosenfeld, G. Salam and V. Sanz, arXiv:1303.6636 [hep-ph].
- [67] CMS Coll. (S. Chatrchyan et al.), JHEP **1111** (2011) 148.
- [68] P. Bartalini and L. Fanò, arXiv:1103.6201 [hep-ex].
- [69] P. Skands and K. Wraight, Eur. Phys. J. C **71** (2011) 1628.
- [70] M. Deak, F. Hautmann, H. Jung and K. Kutak, Eur. Phys. J. C **72** (2012) 1982; arXiv:1112.6386 [hep-ph].
- [71] F. Hautmann, arXiv:1205.5411 [hep-ph].
- [72] M. Garcia-Echevarria, A. Idilbi and I. Scimemi, JHEP **1207** (2012) 002; Phys. Rev. D **84** (2011) 011502; J.-Y. Chiu, A. Jain, D. Neill and I.Z. Rothstein, JHEP **1205** (2012) 084; T.C. Rogers, arXiv:1304.4251 [hep-ph]; P.J. Mulders and T.C. Rogers, Phys. Rev. D **81** (2010) 094006; S. Mantry and F. Petriello, Phys. Rev. D **84** (2011) 014030; Phys. Rev. D **83** (2011) 053007; Y. Li, S. Mantry and F. Petriello, Phys. Rev. D **84** (2011) 094014; A. Jain, M. Procura and W.J. Waalewijn, JHEP **1204** (2012) 132; T. Becher and M. Neubert, Eur. Phys. J. C **71** (2011) 1665; I.W. Stewart, F.J. Tackmann and W.J. Waalewijn, JHEP **1009** (2010) 005; F.A. Ceccopieri, Mod. Phys. Lett. A **24** (2009) 3025; I. Cherednikov and N. Stefanis, arXiv:1104.0168 [hep-ph]; Phys. Rev. D **80** (2009) 054008; Mod. Phys. Lett. A **24** (2009) 2913; Nucl. Phys. B **802** (2008) 146; Phys. Rev. D **77** (2008) 094001; J.C. Collins and F. Hautmann, JHEP **0103** (2001) 016; Phys. Lett. B **472** (2000) 129; F. Hautmann, Nucl. Phys. B **604** (2001) 391; arXiv:0708.1319; hep-ph/0011381; hep-ph/0105098; hep-ph/0101006.

- [73] F. Dominguez, J.W. Qiu, B.W. Xiao and F. Yuan, Phys. Rev. **D85** (2012) 045003; F. Dominguez, A.H. Mueller, S. Munier and B.W. Xiao, Phys. Lett. **B705** (2011) 106; B.W. Xiao and F. Yuan, Phys. Rev. **D82** (2010) 114009; Phys. Rev. Lett. **105** (2010) 062001; F. Dominguez, B.W. Xiao and F. Yuan, arXiv:1009.2141 [hep-ph]; F. Hautmann and D.E. Soper, Phys. Rev. **D75** (2007) 074020; Phys. Rev. **D63** (2000) 011501; F. Hautmann, arXiv:0812.2873 [hep-ph]; Phys. Lett. **B643** (2006) 171; hep-ph/0209320; hep-ph/0105082; F. Hautmann, Z. Kunszt and D.E. Soper, hep-ph/9906284; hep-ph/9806298.
- [74] M. Hentschinski and C. Salas, arXiv:1301.1227 [hep-ph].
- [75] E. Dobson (ATLAS Coll.), presented at MPI@TAU, October 2012; P. Bartalini (CMS Coll.), presented at MPI@TAU, October 2012.
- [76] CMS Coll. (V. Khachatryan et al.), JHEP **1009** (2010) 091.
- [77] A. Grebenyuk et al., Phys. Rev. **D86** (2012) 117501.
- [78] ATLAS Coll. (G. Aad *et al.*), Nature Commun. **2** (2011) 463.
- [79] CMS Collaboration, CMS-PAS-QCD-11-002 .
- [80] CMS Collaboration, CMS-PAS-FWD-11-001 .
- [81] T. Sjöstrand and P. Skands, JHEP **0403** (2004) 053.
- [82] ATLAS Coll. (G. Aad *et al.*), Phys. Rev. D **84** (2011) 054001.
- [83] K. Werner, Iu. Karpenko, M. Bleicher, T. Pierog and S. Porteboeuf-Houssais, Phys. Rev. C **85** (2012) 064907.
- [84] D. d'Enterria and A.M. Snigirev, Phys. Lett. **B718** (2013) 1395.
- [85] M. Strikman, Acta Phys. Polon. B **42** (2011) 2607; T.C. Rogers, A.M Stasto and M.I. Strikman, Phys. Rev. **D77** (2008) 114009.
- [86] G. Gustafson, L. Lönnblad and G. Miu, Phys. Rev. D **67** (2003) 034020; JHEP **0209** (2002) 005; Phys. Rev. D **63** (2001) 034004.
- [87] K. Kutak, W. Placzek and D. Toton, arXiv:1303.0431 [hep-ph]; M. Deak, arXiv:1209.6092 [hep-ph]; K. Kutak, K. Golec-Biernat, S. Jadach and M. Skrzypek, JHEP **1202** (2012) 117.
- [88] Yu.L. Dokshitzer, Acta Phys. Polon. B **36** (2005) 361; hep-ph/9812252.